Quantitative evaluation of range and metabolic activity of hepatic alveolar echinococcosis lesion microenvironment using PET/CT and multi-site sampling method

Abudusalamu Aini (abdusallam925@hotmail.com)
Xinjiang Medical University Affiliated First Hospital https://orcid.org/0000-0002-5633-2317

Maiweilidan Yimingjiang
Xinjiang Medical University Affiliated First Hospital

Aimaiti Yasen
Xinjiang Medical University Affiliated First Hospital

Bo Ran
Xinjiang Medical University Affiliated First Hospital

Tiemin Jiang
Xinjiang Medical University Affiliated First Hospital

Xiaohong Li
Xinjiang Medical University Affiliated First Hospital

Jian Wang
Xinjiang Medical University Affiliated First Hospital

Kasimu Aihaiti
Xinjiang Medical University Affiliated First Hospital

Aisika Ainiwa
Xinjiang Medical University Affiliated First Hospital

Aubuduaini Abulizi
Xinjiang Medical University Affiliated First Hospital

Yingmei Shao
Xinjiang Medical University Affiliated First Hospital

Tuerganaili Aji
Xinjiang Medical University Affiliated First Hospital

Hao Wen
Xinjiang Medical University

Research article

Keywords: alveolar echinococcosis (AE), multi-site sampling (MSS), PET/CT, lesion microenvironment (LME), immune infiltration

Posted Date: August 20th, 2020

DOI: https://doi.org/10.21203/rs.3.rs-18936/v2

Version of Record: A version of this preprint was published at BMC Infectious Diseases on July 23rd, 2021. See the published version at https://doi.org/10.1186/s12879-021-06366-3.

Abstract

Background: Alveolar echinococcosis (AE) lesion microenvironment (LME) is crucial site where parasite-host interactions happen and of great significance during surgery and obtaining liver samples for basic research targeting immunology. However, little is known about quantification of LME range and its' metabolic activity regarding different lesion types.

Methods: A prospective analysis of LME from consecutive surgical AE cases with relevant imaging results was performed. Patients (n=39) received abdominal computed tomography (CT) and position emission tomography/computed tomography using ^{18}F-fluodeoxyglucose (^{18}F-FDG-PET/CT) within one week prior to surgery. Tumor to background ratios (TBRs) of standard uptake value (SUV) in PET/CT was calculated for corresponding LME regions. Multi-site sampling method (MSS, n=26) was introduced to obtain histological slides from LME at different levels off the lesion to evaluate immune cell infiltrative ranges quantitatively. At last, data was statistically analyzed from the perspective of different lesion types.

Results: Altogether six major lesion categories have been identified based on different morphology and calcification pattern (A: non-calcified uniform density lesion; B: diffuse calcified solid lesion; C: half necrotic and half solid lesion with minor calcification; D: half necrotic and half solid lesion with obvious calcification; E: subtotal necrotic lesion with minor calcification; F: total necrotic lesion with obvious calcification). Statistical significances were resulted from TBRs calculation (A>B, A>D, A>F, B<C, B<E, A+C+E>B+D+F, etc.). Less calcified lesions were evidenced with higher TBRs, however, not much was valuable for necrosis. The 95% CI of LME ranges were (10.0, 12.1) mm and (9.9, 14.0) mm by PET/CT and MSS. And, weak regressions between TBRs and LME ranges indicated by PET/CT or MSS (r^2 respectively were 0.2436 and 0.3171) were observed.

Conclusions: PET/CT showed distinct TBRs for different lesion types with heterogenic calcification. PET/CT and MSS had similar discoverability for LME ranges, which also varied among different lesion types. Higher activity meant wider LME range within certain limit. This pioneering study would be able to provide references for both surgical removal of lesions and sample acquisitions more accurately for basic research targeted to immunology.

Background

Human alveolar echinococcosis (AE), caused by the larva stage of *Echinococcus multilocularis* infection, in one of the lethal infectious diseases and causes severe organ damage[1, 2]. Radical resection with negative margin associated with anti-parasitic medication is considered as the best curable options[2-4]. Liver being the predominant target organ (>90%), hepatic AE presents complexity considering the infiltrative growth pattern of the lesion, variant lesion morphology, different clinical stages, distinct biological activity of the parasitic lesion, metabolic activity of the lesion microenvironment (LME). Among prognosis-affecting factors, LME plays significant role.

Moreover, liver resection during surgery and its' accuracy including LME is a potential prognosis-influencing aspect[3]. Besides, sample acquisition from LME liver and adjacent liver tissues (respectively for experimental and control groups) has been introduced to study immunology, fibrosis, pathophysiological changes etc. of the host[5-8]. However, there was no clear evidence for such sampling method that could clearly differentiate the

real experimental and control liver tissues by separating the immune cell infiltrative boundary. And, there is little known about the quantification of standard uptake value (SUV) of ^{18}F-fluodeoxyglucose in position emission tomography/computed tomography (PET/CT) regarding different LME ranges in several heterogenic lesion types.

In this prospective study, we collected surgical hepatic AE subjects' preoperative computed tomography (CT), PET/CT, clinical data, and LME liver samples acquired through multi-site sampling method (MSS). Our primary research results concerning such sampling method for immunological study has been reported as "at least 2 cm distant from lesion" as a method to obtain adjacent normal liver tissue for controls previously[5]. Currently, we finished this prospective study that mainly focused on TBRs' differences and quantification of LME ranges in several lesion categories. Patients were grouped into six types based on lesion parameters focusing on morphology and calcification features. And, SUV data associated with histopathological slides were analyzed to assess the tumor to background ratios (TBRs) of SUV and LME ranges to provide first-hand results of such setting.

Methods

Clinical patient enrollment

During January 2017 to December 2019, hepatic AE patients were evaluated by multidisciplinary team to decide treatment modalities. Inclusion criteria: (i) hepatic AE patients with definitive surgical indications; (ii) patients with both preoperative abdominal CT and ^{18}F-FDG-PET/CT; (iii) patients with enough liver tissue for MSS for pathology during surgery. On the contrary, patients with chronic inflammatory diseases, autoimmune diseases, liver failure (grade Child C), immunocompromised situations, acute cholangitis or hepatitis, severe metabolic disorders were excluded. Subjects with relevant above two imaging examinations but without surgery were included for TBRs analysis.

Abdominal CT

Patients underwent standardized three-phase CT imaging of the liver, including pre-contrast images plus early and late phase images after contrast medium was introduced venously. Scanning was performed using a 64-slice spiral CT machine (GE Lightspeed Ultra, USA). The voltage and current were 120 kV and 300mA. After routine scanning of the whole body, 40-50 ml of Iohexol (300 mg/ml) was injected intravenously using an Ulrich high pressure syringe at a flow velocity of 4.0-4.5 ml/s and a reservation time of 8 seconds. Continuous scanning was done for 55 seconds with 5 mm slice thickness (layer space was 5 mm). Subsequently, images were transferred to an AW4.2 workstation (GE, USA)[9]. All CT images were interpreted as part of the clinical examinations by two experienced radiologists that specialized in abdominal imaging, and a third senior radiological expert was invited for possible bifurcations.

Basic parameters of AE lesions (size and location) and morphological features (density, uniformity, the presence of calcification and its' characteristics) were recorded in detail. Diameter was measured in three dimensions (axis, coronary and sagittal) and average diameter was calculated as representative. Specially, evaluation of calcification and presence of necrosis was graded with three levels for each: (1) calcification (Cal): (-) no evidence of calcification; (+) minor calcification or central calcification without periphery calcification; (++)

diffused or subtotal calcification of the periphery area of the lesion; (2) necrosis (Nec): (-) no evidence of necrosis or uniform lesion; (+) half necrotic half uniform lesion with obvious uniform density area at lesion periphery; (++) almost full necrotic lesion without obvious solid component.

^{18}F-FDG-PET/CT and TBRs

Subjects had whole body ^{18}F-FDG-PET/CT using the Discovery VCT PET/CT (GE Healthcare Bio-Sciences, USA). The tracer ^{18}F-FDG was produced by Cyclotron (GE Healthcare Bio-Sciences, USA) that had a radiochemical purity of >95%. Prior to the examination, patients fasted for at least 6 h to achieve a fasting blood glucose concentration <7 mmol/l. Relevant parameters were: Voltage, 120 kV; tube current, 260 mA; detector collimation, 64×0.625 mm; layer thickness, 3.75 mm; interlayer spacing, 3.75 mm; 0.6 msec/rotation; detector pitch, 0.983; and scanning time, 20-30 sec.

During examination, patients were intravenously injected with ^{18}F-FDG (7.4 MBq/kg body weight) and subjected to take 1,000 ml water orally after 30 min. Further 300 ml water was taken to fill the gut and duodenum following urination with empty bladder. For the next step, positioning images were drawn to determine the scanning range (from the top of the cranium to the mid-upper segment of the thighbone). Patients were educated to breathe smoothly. The three-dimensional PET acquisition was performed with the same scanning range as the CT, generally with 6-8 bed positions. Data for each bed position were collected for 3 min. Then, the CT data were applied to perform attenuation corrections for the PET images. The ordered subset expectation maximization iterative method was used to reconstruct the images of the cross-sectional, coronal and sagittal planes, as well as the PET/CT fusion images[10].

Imaging diagnosis was carried out by two experienced physicians, and the PET, CT and PET/CT fusion images were independently analyzed: image quality was determined by visual analysis, allowing normal physiological uptake, as well as normal variations and artifacts, to be standardized; the abnormal radiopharmaceutical accumulation and biological borders of the lesions, and the numbers and measurements of the maximum standardized uptake value (SUV_{max}) accumulated in these lesions were recorded; average SUV (SUV_{ave}) of background liver at same slice was measured; according to the anatomical information provided by the same CT machine, the position of each lesion was then precisely identified. TBRs was calculated by SUV_{max} / SUV_{ave}. At last, LME ranges were measured at three different sites to calculate the average scales.

Surgery and medical treatment

Patients were operated for hepatic AE after multidisciplinary team evaluation. Main procedures were conventional hepatectomy (minor, major, excessive), hepatectomy associated with vascular reconstruction, and *ex vivo* liver resection and autotransplantation for those contraindicated to conventional therapies[11], and one of them had received auxiliary partial autologous liver transplantation[12]. Post-operatively , all patients were enrolled in regular anti-parasitic medication therapy and followed up routinely according to expert consensus[1, 3].

MSS and pathology

MSS samples were acquired from surgical specimens. The specific sampling site were preoperatively planned through spatial information based on CT and PET/CT, even using three-dimensional reconstruction

techniques[13, 14]. First, liver specimens which contained the target lesion (approximately 1 cm at thickness) as well as adherent liver tissue (at least for 5 cm at length) were cut into size about 2cm*3cm*6cm, and fixed with formalin immediately. Note that, not all cases' liver condition could allow sufficient liver tissue for MSS. For example, (a) left hemi-hepatectomy for left medial lobular lesions could allow MSS due to sufficient left lateral lobular liver parenchyma; (b) left lateral lobectomy for left lateral lobular "full-spaced" lesion could not allow for MSS because of insufficient adherent liver tissue at resection margin. Secondly, after 24-48 h fixation, MSS sampling was performed: liver samples were obtained at parallel levels to lesion surface with 5 mm intervals. Thirdly, paraffin embedded slides were prepared using routine protocols. At last, hematoxylin-eosin (HE) staining and immunohistochemistry for CD3 molecule were performed using manufacturers' protocols. The widest range was defined by the most distant obviously positive CD3 expression level compared to even more distant slides.

Lesion categorization

Lesions were categorized into different groups based on calcification (Cal) and necrosis (Nec) metrics (Fig 1):

(A) non-calcified uniform density lesion: Cal (-), Nec (-);

(B) diffuse calcified solid lesion: Cal (++), Nec (-);

(C) half necrotic and half solid with minor calcification: Cal (+), Nec (+);

(D) half necrotic and half solid with obvious calcification: Cal (++), Nec (+);

(E) subtotal necrotic lesion with minor calcification: Cal (+), Nec (++);

(F) total necrotic lesion with obvious calcification: Cal (++), Nec (++);

A demand for at least three repeats (at least three patients) for each lesion types were set ahead of this study to assure the quality of datasets.

Statistical analysis

TBRs and LME ranges were presented in median with interquartile, and 95% CI were given. One-way ANOVA (Kruskal-Wallis test) and Non-parametric test (Mann Whitney test) were used to determine the significance of TBRs and LME ranges between groups; Non-parametric test (Wilcoxon matched pairs test) was used to compare paired LME ranges indicated by PET/CT and MSS; linear regression was drawn to observe the link of TBRs and LME ranges (r^2 was given). $P < 0.05$ was chosen as standard to judge statistical significance, and actual values were also presented for every test.

Results

Baseline characteristics

From more than 180 surgical hepatic AE cases during study period, 39 patients with 54 lesions finished this study. Median age was 34y (ranging from 15 to 65y), gender ratio (male: female, M/F) was 17/22. Lesion size with average diameter was 11.6 cm (ranging from 4.0-18.0 cm, larger lesion was chosen for multiple lesions in same patient). Lesion location in the liver mainly was right trisection, right lobe, middle lobe and others.

According to expert consensus and recent reviews, PNM stages were I, II, III, and IV, respectively composed by 1, 2, 7, 13 and 16 cases (2.6%, 5.1%, 17.5%, 33.3%, 41.0%) (Table 1). CT and PET/CT were conducted by all subjects which had surgical treatment, and 66.7% (n=26) patients' surgery allowed us to get MSS samples for pathology.

TBRs

TBRs were calculated from three repeats, median value was 3.60 (25% and 75% interquartile were 2.75 and 4.40) for all subjects (95%CI was 3.34-4.45). Comparison between all six lesion types showed apparent significances, including differences of TBRs between different degree of calcification and necrosis. Specifically, non-calcified uniform density lesion (A) had higher TBRs compared to diffuse/obvious calcified (++) groups (B, D, F); diffuse calcified solid lesion (B) had lower TBRs than minor or centrally calcified (+) groups (C, E). Besides, from the perspective of calcification only: non-calcified or minor/central calcified lesions together (A+C+E) had higher TBRs compared to diffuse/obvious calcified groups together (B+D+F) However, from the perspective of necrosis, no statistical significances were observed (P>0.05). More constitutional comparisons could be found in Fig 2.

LME range

LME ranges were measured by PET/CT images and were also confirmed based on MSS slides. Comparisons were performed for each groups and their different constitutions:

(1) LME range indicated by PET/CT: both of the total necrotic lesion with obvious calcification (F) and the half necrotic and half solid with obvious calcified lesion (D) had significant narrower range than non-calcified or minor calcified lesions (A, C, E); from the perspective of calcification and necrosis, different constitutional comparisons were presented in Fig 3.

(2) LME range indicated by MSS: both of the non-calcified uniform density lesion (A) and the half necrotic and half solid with minor calcified lesion (C) had wider range compared to lesion types D and F; from the perspectives of calcification and necrosis, different constitutional comparisons were presented in Fig 4.

(3) Comparison of LME range indicated by PET/CT and MSS: no matter what was the groups or different constitutions regrading different calcification or necrosis degrees, there was not any statistical significance observed between these two methods.

(4) MSS pathology: As an example, pathological slides showed gradually decreased CD3 positive cells in the LME region of type A lesion (Fig 5). The very inside and very outside slides were evidenced with the extremes of immune cell infiltrating levels from the lesion surface.

Regression of TBRs and LME ranges

Most of the values were located at the third quadrant in regression panel. And the regressions for TBRs and LME ranges respectively indicated by PET/CT and MSS revealed weak r^2 values both in all and each group (Fig 6).

Discussion

Chronic and infiltrative growth pattern of AE lesion could result into many manifestations within the liver[4]. We have noticed the spatial heterogeneity of AE lesions at early times, and practiced much from the perspectives of diagnosis, clinical treatment and basic researches. However, the thing has not solved so far that AE lesion categorization based on radiological imaging tools. Obviously, lesion typing could help radiologists, clinicians, parasitologists to precisely evaluate and choose certain management options for patients[15-17]. An AE lesion includes various factors to be evaluated during the whole process: lesion basic or anatomical characteristics (size, location, ect.), morphology (by radiology and pathological view), calcification features (by radiology mostly), lesion biological activity (or parasitic viability), LME metabolic activity (mostly assessed by PET/CT so far), vasculature involvement (both intra- and extra-hepatic vessels including biliary trees, these are also linked with certain comorbidities to be assessed), immunological status of the patients. Among them, LME has core roles form the perspectives of anatomy, radiology, pathophysiology, and immunology.

In the past, several imaging tools demonstrated lesion types for hepatic AE[18-20]. And there were some other imaging methods and researches on comparison of different imaging tools[21-25]. These strategies had proposed new methods for lesion categorization. Nevertheless, no integrative typing system has been established so far, and they were asymmetric when defining clinical stage or lesion activity regarding different lesion types. Besides, among the lesion types that proposed by *Kodama et al*, *Kratzer et al* and *Graeter et al*, there were not clear integrative bridge to definitely link them, and no relevant study which used all these imaging tools in same patient cohort has been reported[18-20]. And this was why we chose to reclassify lesions based on two factors (calcification and necrosis). One of our near future studies will focus on lesion typing specifically, and will discuss about the drawbacks of each tools and optional typing system. At present, professionals have come to the conclusion that PET/CT is the valuable tool to asses lesion activity and seems to be an unreplaceable imaging method.

In current study, we assessed TBRs regarding different lesion types, which was based on distinct calcification and necrosis. These types were further evidenced with gross specimens and microscopic analysis. Our results showed that there were significant TBRs differences between different lesion types, as well as different degree of calcification. Apparently, less calcified lesions had higher TBRs although there were no differences between any degree of necrosis. The higher TBRs value is, the stronger the lesion activity. At the meantime, calcification and necrosis could be evaluated by CT easily. So, TBRs value can be correlated to corresponding lesion types to help professionals to decide which treatment option would be best.

When it came to LME range (^{18}F-FDG uptake region around the lesion), PET/CT and MSS presented no obvious differences no matter which lesion type it was. Interestingly, LME ranges also varied between different lesion types. Generally, less calcification and necrosis meant wider LME range. Although, it is understandable that calcification and necrosis are the ways of death of the parasitic lesion, but, differential degrees of calcification and necrosis as well as integration of them had revealed further insights of AE lesions. In addition, regression between TBRs and LME range indicated by PET/CT and MSS were weak to conclude the relations. It is worth to point out that, even the TBRs is very high, LME range could not be symmetrically wide, because parasitic-host interactions need close contact, and the longer the distance is, the harder the enrichment of host cells or other parenchymal components happen.

Moreover, the LME region may directly affect the experimental outcome when not balanced properly by mimicking real experimental liver tissue with the real control liver tissues. A previous research has studied

surrogate markers in distinguishing metabolically active and inactive AE patients[26]. In this study, methodology for sampling was defined as “specimens were taken from the AE lesion area and from a macroscopically normal distant area of liver tissue”, however, the precise area has not been described, but there was a well consideration for control liver tissue acquisition based on pathology. Another recent study sampled the liver tissues with 2 cm line to study Kupffer cell and fibrosis in hepatic AE[7]. Also, no specific leison type heterogeniety was decribed except expressiong that “the liver tissues were taken within 2 cm of the lesion by surgery for the close group, whereas the liver tissues were taken 2 cm outside the lesion for the distance group”. If a 2 cm line has to be chosen to determine the experimental and control liver tissues: (a) it would definitely reduce both of the targeted immune cell number and cell types in cases with narrower LME range than 2 cm; (b) it would also increase them in cases with wider LME range that 2 cm. Meanwhile, some other studies never layed out the sampling areas or scales[27]. Of course, it was major result-influencing factor. So, we strongly recommend that the differentiative line should be based on different lesion types to achieve best performance of liver-based studies for AE.

The potential for resection and whether there is disease dissemination must be assessed carefully by pre-operative imaging techniques[3]. Surgical removal of parasitic lesion plus peri-lesion inflammatory belt is recommended. A western study demonstrated that R0 resection had 2% disease recurrence, whereas, R1 and R2 resections showed 41% of intrahepatic disease progression during follow-up[28]. Another study reported late recurrence even after R0 resection[29]. It also emphasized the importance of R0 resection of AE lesion. However, how wide the peri-lesion inflammatory belt (corresponding to LME) has not been studied based on distinct lesion types. Besides, achieving 2 cm resection margin for every single lesion is not possible in most advanced cases as recommended[3, 4, 28, 30]. For excessive vascular infiltrated lesion or with severe comorbidities, only liver transplantation or *ex vivo* liver resection and autotransplantation could be selected from the perspective surgical treatment[11, 31-40]. Our data indicated that, different lesion types had different immune cell infiltrated belt. For major/obvious calcified lesions, less than 2 cm resection margin would be satisfactory; for severe necrotic lesion with obvious calcified capsule, less than 1 cm resection margin will be enough. Extra indications for resection margin could also be concluded from this study results.

Objectively speaking, shortcomings of this study were that we were short when enrolling patients which had both PET/CT and MSS data because of different surgical approaches (not all surgeries could provide sufficient liver samples), and some other lesion categories were not included due to unavailability of PET/CT or MSS. Moreover, MSS with 5mm intervals off the lesion shore prevented us to map the immune cell infiltration with higher resolution. Further, methodology for simulating every spatial SUV digital data would be more helpful to understand the spatial heterogeneity of a lesion. Future insights of LME should be discovered in depth in further researches.

Conclusions

This pioneering study would be able to provide references for both surgical removal of lesions and sample acquisitions more accurately for basic research targeted to immunology and pathophysiological changes of LME. PET/CT and MSS had similar discoverability for LME ranges, which varies among different lesion types. Higher activity meant wider range of LME within certain limit: non-calcified uniform density lesion had higher TBRs (median 4.4, ranging from 3.7-7.0) than other lesions and median 13mm (ranging from 10-20mm) LME

range; obvious calcified or central necrotic lesions had had variant TBRs (ranging from 1.7-6.4) and LME ranges (ranging from 7-13mm). Sample acquisition based on different lesion types were strongly advised for certain experimental and control studies.

Declarations

Ethics approval and consent to participate

All procedures were performed in adherence to the terms of the latest version of the Declaration of Helsinki for Medical Research involving Human Subjects and approved by the Ethical Committee of the First Affiliated Hospital of Xinjiang Medical University. All included patients were provided with written informed consent for anonymous collection and analysis of clinical data was provided by all patients before surgery in this retrospective cohort. For patients under 18 year-old, writen informed consent was also obtained from parent/guardian and this was also has been approved by the Ethical Committee of the First Affiliated Hospital of Xinjiang Medical University.

Consent for publication

All patients signed written informed consent for publication of relevant data.

Availability of data and materials

The datasets used/analyzed during the current study are within the manuscript, and further data could be available from the corresponding author on reasonable requests.

Competing interests

The authors declare no conflict of interest regarding this manuscript.

Funding

National Natural Science Foundation of China (No. 81660108, 81960377 to Prof. Tuerganaili Aji) and National Major Science and Technology Project of China (No. 2018ZX10301201 to Prof. Tuerganaili Aji) financially supported this study from design to submission process, including costs for patient follow-ups as well as students' remuneration who joined study performance. All authors together declare that there was no other financial compete to disclose.

Authors' contributions

AAini designed the MSS sampling method, acquired clinical and imaging data, drafted and revised the manuscript, analyzed and presented the data; MY and AY performed pathological experiments and analyzed the data; BR and TJ participated in surgeries and offered guidance in data acquisition; XL and JW participated in radiological & nuclear medical examinations and offered help in data acquisition; KA, AAiniwa and AAbulizi acquired clinical and imaging data; YS, TA and HW performed the surgeries and supervised during the study; YS and TA interpreted and analyzed the data; TA acquired funds and critically revised the manuscript; HW

conceived and designed the whole study, conceptualized the MSS sampling method, revised the manuscript and approved for publication;

Acknowledgements

Not applicable.

Supplementary materials

This study included seven supplementary materials related to figures and table in the text, and they could be found online.

Abbreviations

AE= alveolar echinococcosis, LME= lesion microenvironment, PET/CT= position emission tomography and computed tomography, MSS= multi-site sampling method, TBRs= tumor to background ratios, SUV= standard uptake value, ^{18}F-FDG= ^{18}F-fluodeoxyglucose, RL= right lobe of the liver, RTS= right trisection of the liver, LTS= left trisection of the liver, LLL= left lateral lobe of the liver, ML= medial lobe of the liver, RPL= right posterior lobe of the liver, R0 resection= radial resection with confirmative negative margin.

References

1. Wen H, Vuitton L, Tuxun T, Li J, Vuitton DA, Zhang W, McManus DP: Echinococcosis: Advances in the 21st Century. Clinical microbiology reviews 2019, 32(2).
2. Deplazes P, Rinaldi L, Alvarez Rojas CA, Torgerson PR, Harandi MF, Romig T, Antolova D, Schurer JM, Lahmar S, Cringoli G, Magambo J, Thompson RC, Jenkins EJ: Global Distribution of Alveolar and Cystic Echinococcosis. Advances in parasitology 2017, 95:315-493.
3. Brunetti E, Kern P, Vuitton DA: Expert consensus for the diagnosis and treatment of cystic and alveolar echinococcosis in humans. Acta tropica 2010, 114(1):1-16.
4. Kern P: Clinical features and treatment of alveolar echinococcosis. Current opinion in infectious diseases 2010, 23(5):505-512.
5. Zhang C, Lin R, Li Z, Yang S, Bi X, Wang H, Aini A: Immune Exhaustion of T Cells in Alveolar Echinococcosis Patients and Its Reversal by Blocking Checkpoint Receptor TIGIT in a Murine Model. 2019.
6. Ricken FJ, Nell J, Gruner B, Schmidberger J, Kaltenbach T, Kratzer W, Hillenbrand A, Henne-Bruns D, Deplazes P, Moller P, Kern P, Barth TFE: Albendazole increases the inflammatory response and the amount of Em2-positive small particles of Echinococcus multilocularis (spems) in human hepatic alveolar echinococcosis lesions. 2017, 11(5):e0005636.
7. Liu Y, Tian F, Shan J, Gao J, Li B, Lv J, Zhou X, Cai X, Wen H, Ma X: Kupffer Cells: Important Participant of Hepatic Alveolar Echinococcosis. Frontiers in cellular and infection microbiology 2020, 10:8.
8. Feng N, Zhang C, Cao W, Peng S, Jiang T, Liu Y, Shang X, Wen H, Ding J, Ma X: CD19(+)CD24(hi)CD38(hi) Regulatory B cells Involved in Hepatic Alveolar Hydatid Infection in Humans. Annals of clinical and laboratory science 2019, 49(3):338-343.

9. Li H, Song T, Qin Y, Liu W, Li X, Shao Y, Wen H: Efficiency of liposomal albendazole for the treatment of the patients with complex alveolar echinococcosis: a comparative analysis of CEUS, CT, and PET/CT. Parasitology research 2015, 114(11):4175-4180.
10. Qin Y, Li X, Zhang Q, Xie B, Ji X, Li Y, Yiblayan A, Wen H: Analysis of the clinical value of (18)F-FDG PET/CT in hepatic alveolar echinococcosis before and after autologous liver transplantation. Experimental and therapeutic medicine 2016, 11(1):43-48.
11. Aji T, Dong JH, Shao YM, Zhao JM, Li T, Tuxun T, Shalayiadang P, Ran B, Jiang TM, Zhang RQ, He YB, Huang JF, Wen H: Ex vivo liver resection and autotransplantation as alternative to allotransplantation for end-stage hepatic alveolar echinococcosis. Journal of hepatology 2018, 69(5):1037-1046.
12. Aini A, Shao Y, Shalayiadang P, Ran B, Jiang T, Zhang R, Aji T, Wen H: Auxiliary Partial Autologous Liver Transplantation for High-selective Alveolar Echinococcosis: A Proof of Concept. Transplantation 2019.
13. He YB, Bai L, Aji T, Jiang Y, Zhao JM, Zhang JH, Shao YM, Liu WY, Wen H: Application of 3D reconstruction for surgical treatment of hepatic alveolar echinococcosis. World journal of gastroenterology 2015, 21(35):10200-10207.
14. He YB, Bai L, Jiang Y, Ji XW, Tai QW, Zhao JM, Zhang JH, Liu WY, Wen H: Application of a Three-Dimensional Reconstruction Technique in Liver Autotransplantation for End-Stage Hepatic Alveolar Echinococcosis. Journal of gastrointestinal surgery : official journal of the Society for Surgery of the Alimentary Tract 2015, 19(8):1457-1465.
15. Schmidberger J, Steinbach J, Schlingeloff P, Kratzer W, Gruner B: Surgery versus conservative drug therapy in alveolar echinococcosis patients in Germany - A health-related quality of life comparison. Food and waterborne parasitology (Online) 2019, 16:e00057.
16. Yang C, He J, Yang X, Wang W: Surgical approaches for definitive treatment of hepatic alveolar echinococcosis: results of a survey in 178 patients. 2019, 146(11):1414-1420.
17. , Qu, and, Y., Lv, and, X.W., Ji, and, B.: 488 MANAGEMENT OF ADVANCED HEPATIC ALVEOLAR ECHINOCOCCOSIS.
18. Kodama Y, Fujita N, Shimizu T, Endo H, Nambu T, Sato N, Todo S, Miyasaka K: Alveolar echinococcosis: MR findings in the liver. Radiology 2003, 228(1):172-177.
19. Kratzer W, Gruener B, Kaltenbach TE, Ansari-Bitzenberger S, Kern P, Fuchs M, Mason RA, Barth TF, Haenle MM, Hillenbrand A, Oeztuerk S, Graeter T: Proposal of an ultrasonographic classification for hepatic alveolar echinococcosis: Echinococcosis multilocularis Ulm classification-ultrasound. World journal of gastroenterology 2015, 21(43):12392-12402.
20. Graeter T, Kratzer W, Oeztuerk S, Haenle MM, Mason RA, Hillenbrand A, Kull T, Barth TF, Kern P, Gruener B: Proposal of a computed tomography classification for hepatic alveolar echinococcosis. World journal of gastroenterology 2016, 22(13):3621-3631.
21. Jiang Y, Li J, Wang J, Xiao H, Li T, Liu H, Liu W: Assessment of Vascularity in Hepatic Alveolar Echinococcosis: Comparison of Quantified Dual-Energy CT with Histopathologic Parameters. PloS one 2016, 11(2):e0149440.
22. Zhang H, Liu ZH, Zhu H, Han Y, Liu J, Deng LQ: Analysis of contrast-enhanced ultrasound (CEUS) and pathological images of hepatic alveolar echinococcosis (HAE) lesions. European review for medical and pharmacological sciences 2016, 20(10):1954-1960.

23. Abudureheman Y, Wang J, Liu W: Comparison of Intravoxel Incoherent Motion Diffusion-Weighted Magnetic Resonance (MR) Imaging to T1 Mapping in Characterization of Hepatic Alveolar Echinococcosis. Medical science monitor : international medical journal of experimental and clinical research 2017, 23:6019-6025.
24. Zheng J, Wang J, Zhao J, Meng X: Diffusion-Weighted MRI for the Initial Viability Evaluation of Parasites in Hepatic Alveolar Echinococcosis: Comparison with Positron Emission Tomography. Korean J Radiol 2018, 19(1):40-46.
25. Brumpt E, Blagosklonov O, Calame P, Bresson-Hadni S, Vuitton DA, Delabrousse E: AE hepatic lesions: correlation between calcifications at CT and FDG-PET/CT metabolic activity. Infection 2019, 47(6):955-960.
26. Tuxun T, Apaer S, Ma HZ, Zhao JM, Lin RY, Aji T, Shao YM, Wen H: Plasma IL-23 and IL-5 as surrogate markers of lesion metabolic activity in patients with hepatic alveolar echinococcosis. Scientific reports 2018, 8(1):4417.
27. Ren B, Wang H, Ren L, Yangdan C, Zhou Y, Fan H, Lv Y: Screening for microRNA-based diagnostic markers in hepatic alveolar echinococcosis. Medicine 2019, 98(37):e17156.
28. Joliat GR, Melloul E, Petermann D, Demartines N, Gillet M, Uldry E, Halkic N: Outcomes After Liver Resection for Hepatic Alveolar Echinococcosis: A Single-Center Cohort Study. World journal of surgery 2015, 39(10):2529-2534.
29. Ammann RW, Renner EC, Gottstein B, Grimm F, Eckert J, Renner EL: Immunosurveillance of alveolar echinococcosis by specific humoral and cellular immune tests: long-term analysis of the Swiss chemotherapy trial (1976-2001). Journal of hepatology 2004, 41(4):551-559.
30. Salm LA, Lachenmayer A, Perrodin SF, Candinas D, Beldi G: Surgical treatment strategies for hepatic alveolar echinococcosis. Food and waterborne parasitology (Online) 2019, 15:e00050.
31. Kamiyama T: Recent advances in surgical strategies for alveolar echinococcosis of the liver. Surgery today 2019.
32. Aliakbarian M, Tohidinezhad F, Eslami S, Akhavan-Rezayat K: Liver transplantation for hepatic alveolar echinococcosis: literature review and three new cases. Infectious diseases (London, England) 2018, 50(6):452-459.
33. Yang X, Qiu Y, Huang B, Wang W, Shen S, Feng X, Wei Y, Lei J, Zhao J, Li B, Wen T, Yan L: Novel techniques and preliminary results of ex vivo liver resection and autotransplantation for end-stage hepatic alveolar echinococcosis: A study of 31 cases. American journal of transplantation : official journal of the American Society of Transplantation and the American Society of Transplant Surgeons 2018, 18(7):1668-1679.
34. Qu B, Guo L, Sheng G, Yu F, Chen G, Wang Y, Shi Y, Zhan H, Yang Y, Du X: Management of Advanced Hepatic Alveolar Echinococcosis: Report of 42 Cases. The American journal of tropical medicine and hygiene 2017, 96(3):680-685.
35. Wen H, Dong JH, Zhang JH, Duan WD, Zhao JM, Liang YR, Shao YM, Ji XW, Tai QW, Li T, Gu H, Tuxun T, He YB, Huang JF: Ex Vivo Liver Resection and Autotransplantation for End-Stage Alveolar Echinococcosis: A Case Series. American journal of transplantation : official journal of the American Society of Transplantation and the American Society of Transplant Surgeons 2016, 16(2):615-624.
36. Wen H, Dong JH, Zhang JH, Zhao JM, Shao YM, Duan WD, Liang YR, Ji XW, Tai QW, Aji T, Li T: Ex vivo liver resection followed by autotransplantation for end-stage hepatic alveolar echinococcosis. Chinese medical journal 2011, 124(18):2813-2817.

37. Aydinli B, Ozturk G, Arslan S, Kantarci M, Tan O, Ahiskalioglu A, Ozden K, Colak A: Liver transplantation for alveolar echinococcosis in an endemic region. Liver transplantation : official publication of the American Association for the Study of Liver Diseases and the International Liver Transplantation Society 2015, 21(8):1096-1102.
38. Kantarci M, Pirimoglu B, Aydinli B, Ozturk G: A rare reason for liver transplantation: hepatic alveoloar echinococcosis. Transplant infectious disease : an official journal of the Transplantation Society 2014, 16(3):450-452.
39. Bresson-Hadni S, Koch S, Miguet JP, Gillet M, Mantion GA, Heyd B, Vuitton DA: Indications and results of liver transplantation for Echinococcus alveolar infection: an overview. Langenbeck's archives of surgery 2003, 388(4):231-238.
40. Hand J, Huprikar S: Liver transplantation for alveolar echinococcosis: Acceptable when necessary but is it preventable? Liver transplantation : official publication of the American Association for the Study of Liver Diseases and the International Liver Transplantation Society 2015, 21(8):1013-1015.

Table

Table 1. Patient demographics, lesion features, surgical approach and MSS cases.

Type	Definition		No	M/F	Age*	Size (cm)*	Location**	Stage (I/II/IIIa/IIIb/IV)	MSS cases
	Calcification degree	Necrotic severity							
A	(-)	(-)	7	3/4	36 (24-47)	11.6 (4.7-18.0)	RTS (3), RL (3), LLL (1), LTS (1),	0/2/0/1/4	5
B	(++)	(-)	7	4/3	41 (27-65)	7.6 (6.1-12.6)	RTS (3), RL (1), ML (3)	1/0/3/1/2	3
C	(+)	(+)	10	5/5	32 (15-53)	12.9 (9.5-15.7)	RTS (3), ML (3), LL (2), LLL (2), LTS (1), RPL (1)	0/0/3/4/3	8
D	(++)	(+)	5	2/3	31 (26-57)	12.0 (8.0-14.9)	RTS (4), ML (1)	0/0/0/4/1	3
E	(+)	(++)	5	1/4	36 (29-52)	14.7 (11.0-17.0)	RTS (3), RL (2)	0/0/1/1/3	4
F	(++)	(++)	5	2/3	33 (26-43)	12.5 (4.0-15.5)	RTS (1), RL (1), LL (2), LTS (1),	0/0/0/2/3	3
Total			39	17/22	34 (15-65)	11.6 (4.0-18.0)	RTS (12), RL (7), ML (7), LL (4), LLL (3), LTS (3), RPL (1)	1/2/7/13/16	24

Note: M/F=male/female ratio; * Median with maximum/minimum ranges were showed (Larger size was presented for multiples lesions); ** In brackets were number of patients; RL=right lobe;

RTS= right trisection; LTS=left trisection; LLL=left lateral lobe; ML=medial lobe; RPL=right posterior lobe.

Figures

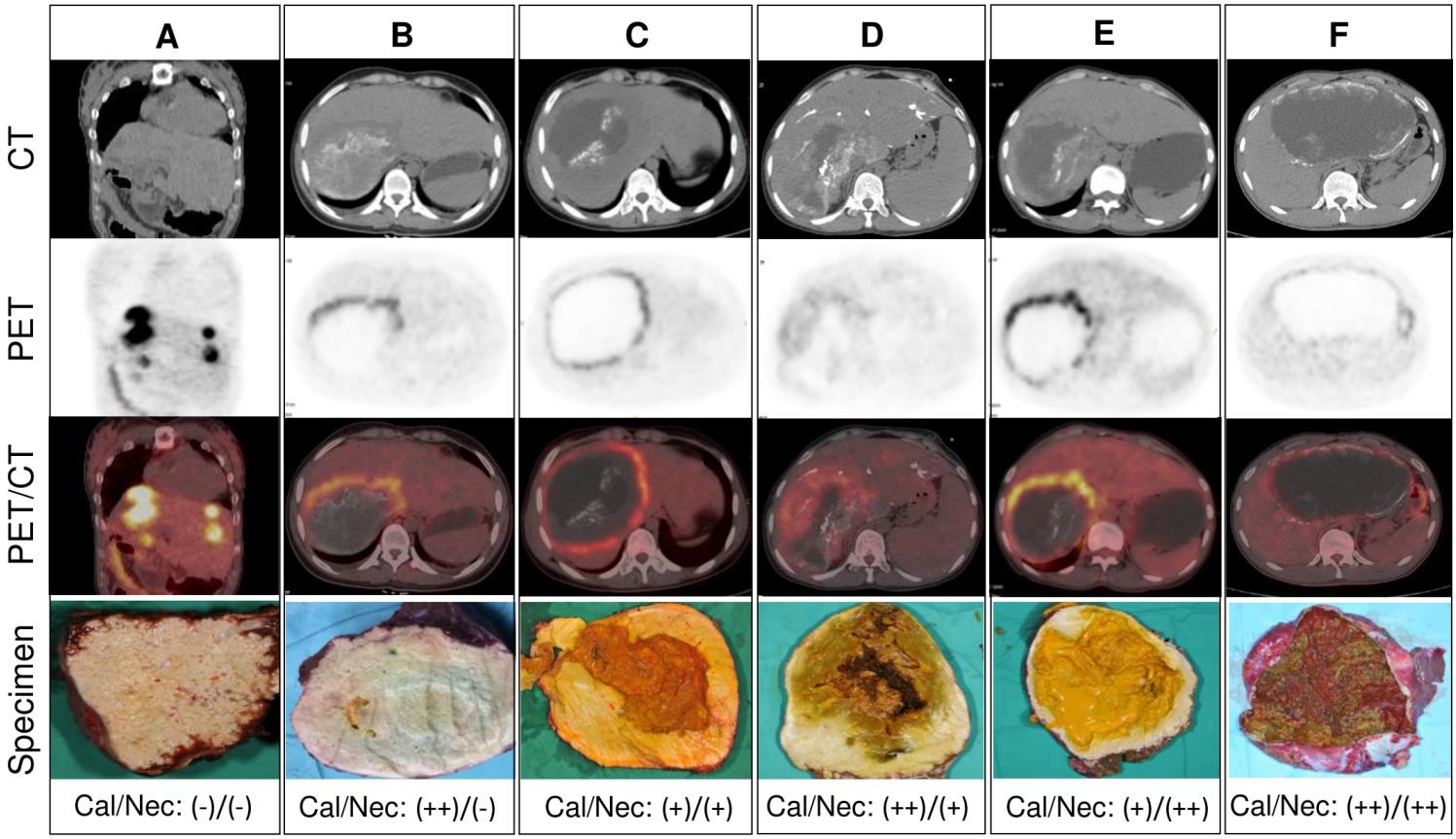

Figure 1

Preoperative PET/CT imaging, gross specimen for different lesion types. Lesions were divided into six groups according to three levels of calcification (Cal) and necrosis (Nec) both ranging from (-), (+), and (++) for each. (A) Uniform density lesion without observable calcification (-) or central necrotic area (-); (B) Uniform solid lesion with obvious diffused calcification (++) and without necrosis (-); (C) Half central necrotic (+) with central circumscribed calcified (+) and outer periphery non-calcified lesion; (D) Half central necrotic (+) with obvious diffused calcified (++) lesion; (E) Central limited calcified (+) and subtotal necrotic (++) lesion; (F) Capsule wall obvious subtotal calcified (++) and subtotal necrotic (++) lesion.

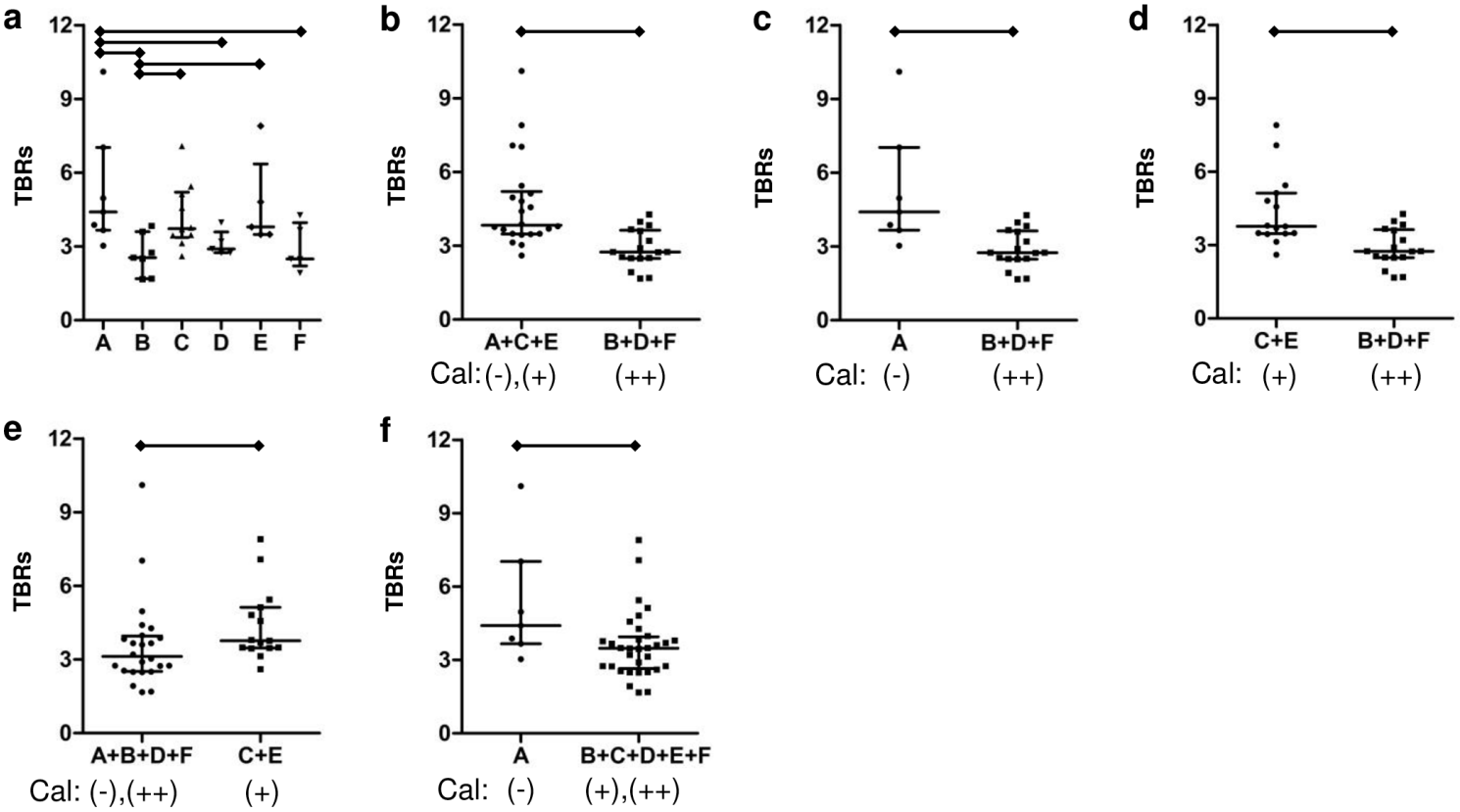

Figure 2

TBRs by in different lesion types. TBRs compared between all lesion types and in accordance with different levels of Cal and Nec. (a) Statistical differences of TBRs between all lesion types; (b)-(f) showed results of constitutional comparisons (also refer to Supplementary material 3).

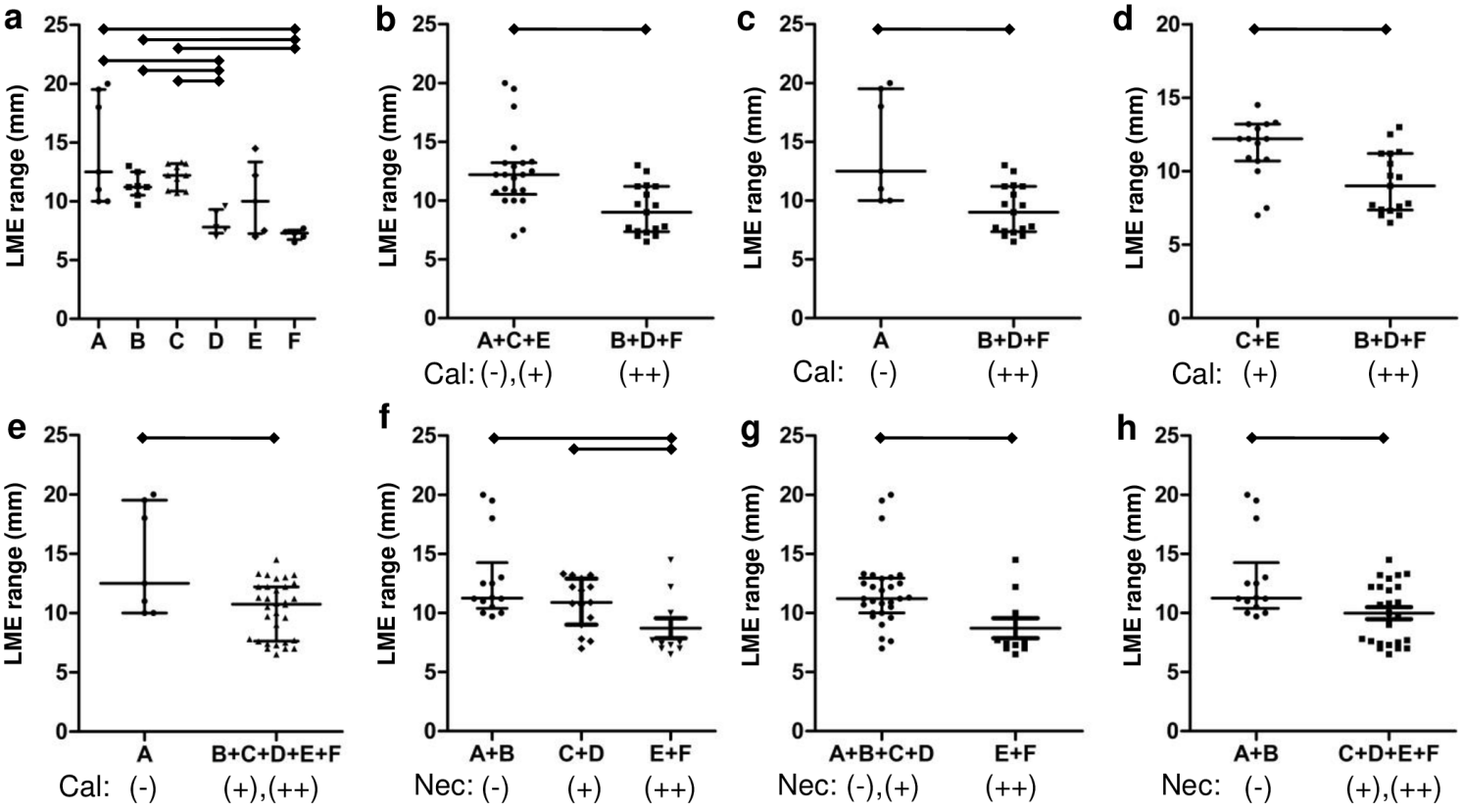

Figure 3

LME range indicated by PET/CT. LME ranges compared between all lesion types and in accordance with different levels of Cal and Nec. (a) Statistical significance of range values between all lesion types; (b)-(h) showed results of constitutional comparisons (also refer to Supplementary material 4).

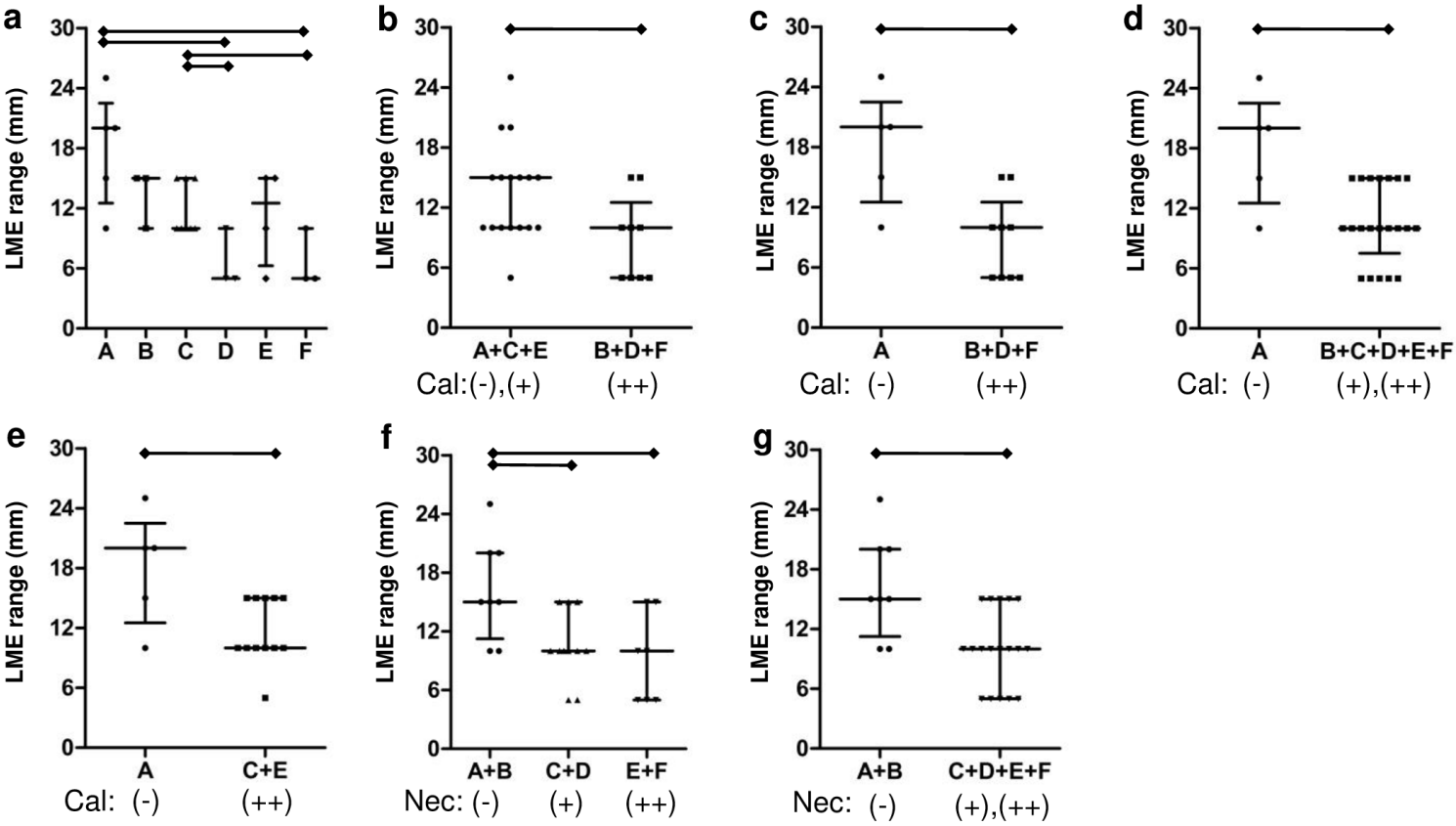

Figure 4

LME range indicated by MSS. LME ranges compared between all lesion types and in accordance with different levels of Cal and Nec. (a) Statistical significance of range values between all lesion types; (b)-(g) showed results of constitutional comparisons (also refer to Supplementary material 5).

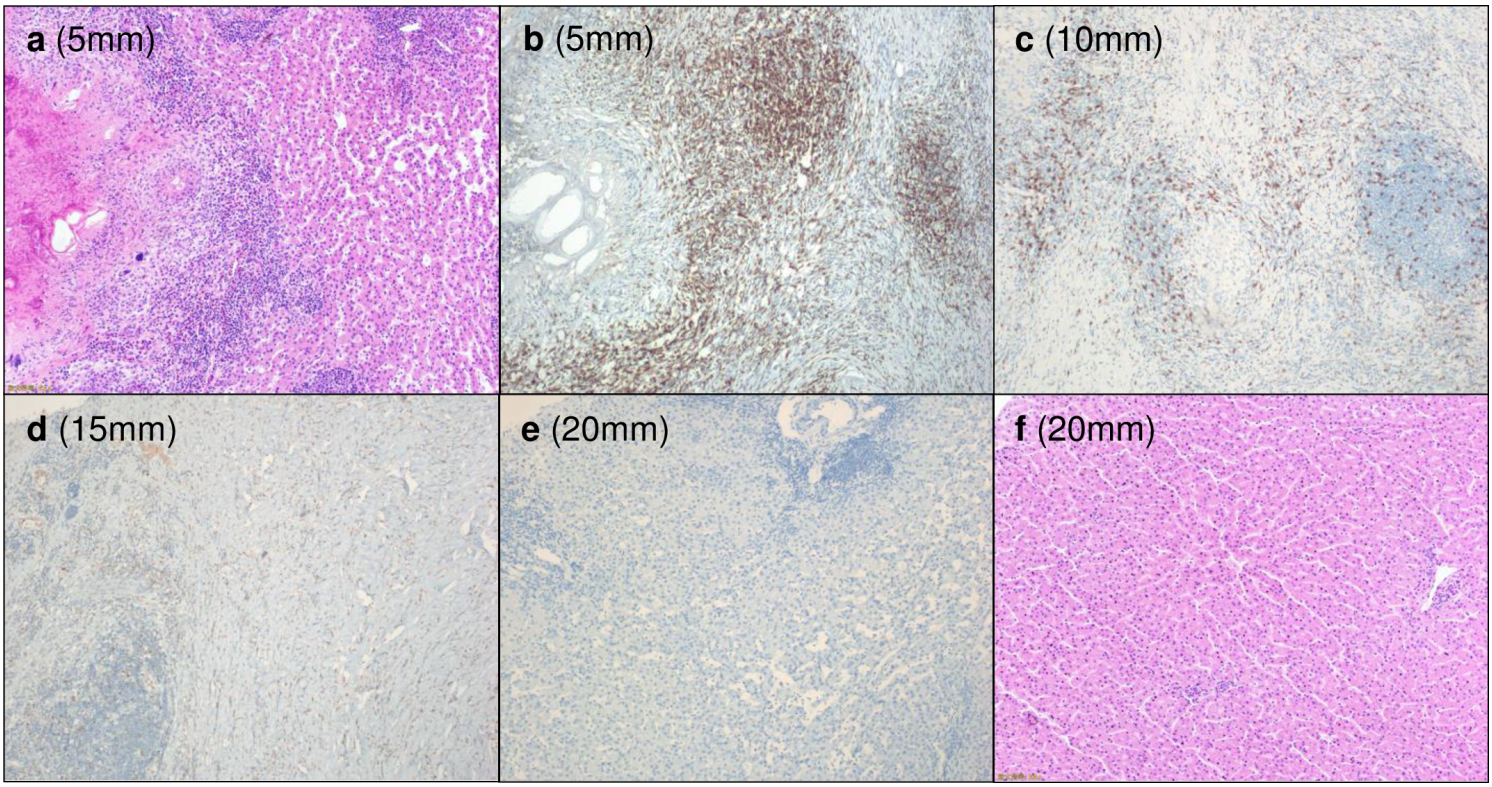

Figure 5

Histopathological presentations of LME in type A lesion at different levels from lesion shore. HE staining (a, f) and immunohistochemistry staining for CD3 molecule at levels of 5, 10, 15, and 20 mm off the lesion shore. From (b) to (e), immune cell infiltration gradually decreased and became inapparent, indicating that at least 15mm was essential when choosing a liver sample as control.

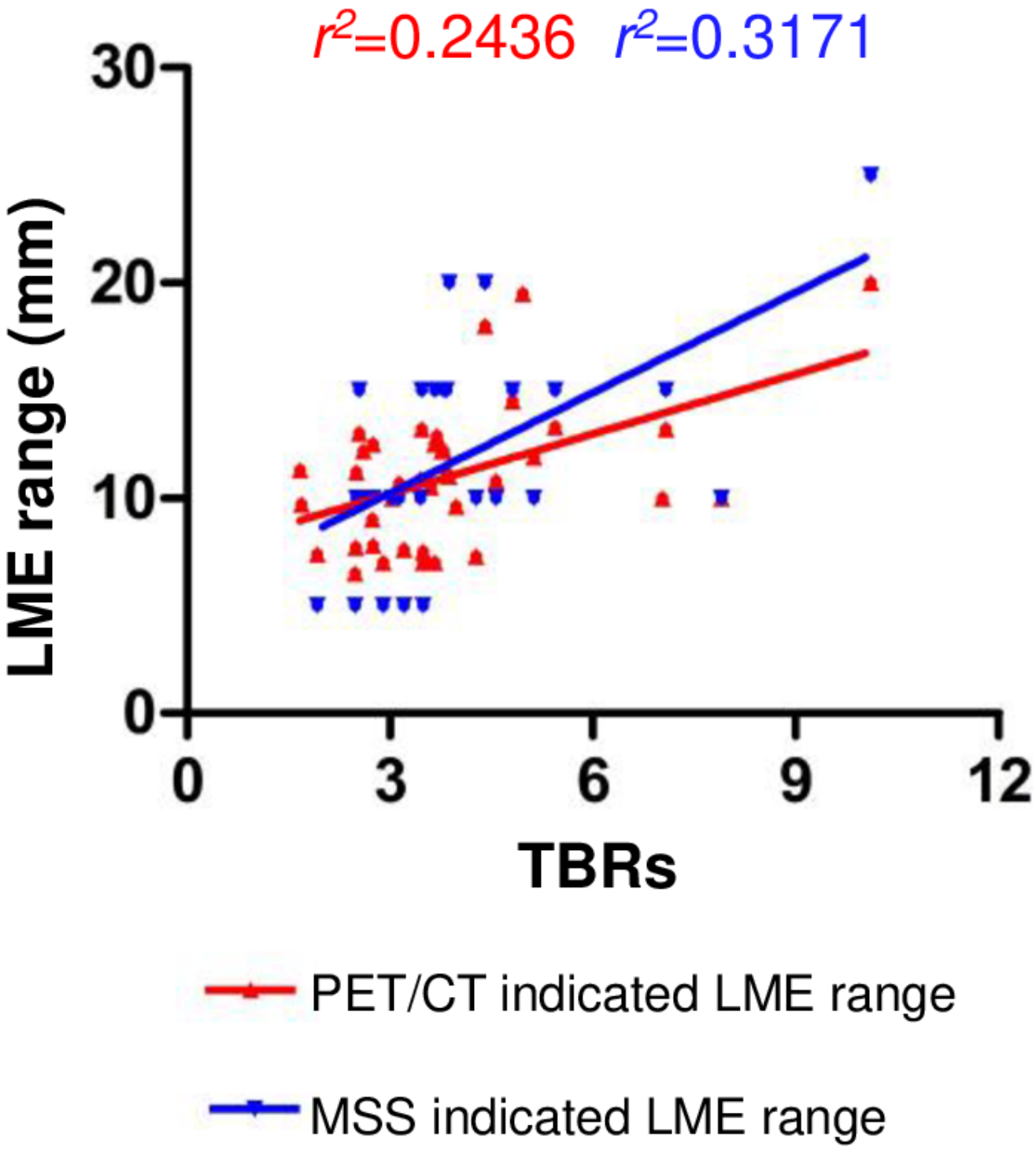

Figure 6

Regressions of TBRs and LME ranges indicated by PET/CT and MSS. Both PET/CT and MSS presented weak linear correlations of TBRs and LME ranges (also refer to Supplementary material 7).

Supplementary Files

This is a list of supplementary files associated with this preprint. Click to download.

- Supplementarymaterials.docx